

Crystalline structure of mixed $\text{Ga}_{1-x}\text{Al}_x\text{As}$ and $\text{GaP}_{1-x}\text{As}_x$ crystals

M. Teicher and R. Beserman

Solid State Institute and Physics Department, Technion—Israel Institute of Technology, Haifa, 32000 Israel

M. V. Klein

Department of Physics, Materials Research Laboratory, and Coordinated Science Laboratory, University of Illinois at Champaign—Urbana, Urbana, Illinois 61801

H. Morkoç

Coordinated Science Laboratory, University of Illinois at Champaign—Urbana, Urbana, Illinois 61801

(Received 4 November 1982; revised manuscript received 24 June 1983)

Two-phonon processes have been used to study the crystalline structure of two mixed-crystal systems. The two-phonon spectra of $\text{Ga}_{1-x}\text{Al}_x\text{As}$ show coupled optical zone-edge phonons, which are GaAs-like, AlAs-like, and also combinations of GaAs-like and AlAs-like zone-edge phonons. The latter combination is not observed in $\text{GaP}_{1-x}\text{As}_x$, the other mixed-crystal system studied here, where the linewidth of the GaP-like Raman mode increases and the Raman intensity rapidly decreases with increasing As content. We explain these results qualitatively by assuming a random distribution of Ga and Al atoms in $\text{Ga}_{1-x}\text{Al}_x\text{As}$ crystals, and a distortion of the lattice structure as well as a departure from a random distribution of atoms in $\text{GaP}_{1-x}\text{As}_x$.

I. INTRODUCTION

The vibrational properties of mixed crystals have been intensively studied in the past 15 years.¹ Most of the attention has been devoted to the description and to the understanding of the properties of phonons at the zone center of the virtual crystal [zone-center phonons (ZCP's)].² Less effort has been spent studying two-phonon spectra, where the density of states favors near zone-edge phonons (ZEP's) firstly, because the experimental second-order Raman scattering (RS) spectrum is usually more difficult to obtain than the first-order one and secondly, because the second-order RS is a higher-order process in the Hamiltonian, and thus more difficult to treat theoretically. ZEP's in an $AB_{1-x}C_x$ lattice have short-wavelength displacements which should be sensitive to such structural details as whether the *B* and *C* atoms are distributed randomly³ or in the form of clusters.⁴ In a mixed crystal, two types of vibrational features are often observed: (1) zone-center Raman or infrared-active modes obeying the selection rules and *k* conservation of the "average" structure and (2) disorder-induced Raman spectra due to a breakdown of the *k* conservation.⁵⁻⁷

Recently there has been a renewed interest in the study of the crystalline structure of mixed crystals. From the photoluminescence of $\text{GaP}_{1-x}\text{As}_x$ it has been inferred that local fluctuations in the composition of the alloys are sufficiently strong to produce a peak due to excitons trapped by the fluctuation in the random potential.⁸ No such peak has been seen in $\text{Ga}_{1-x}\text{Al}_x\text{As}$.⁹ This trend is in accordance with the infrared reflectivity study on the latter system which shows the existence of two structureless restrahlen bands only.¹⁰

From x-ray data we know that mixed crystals behave like virtual crystals to the extent that the lattice mean

spacing follows Vegard's law. But it has been shown recently, using extended x-ray-absorption fine-structure (EXAFS) techniques, that in solid solutions of $\text{Ga}_{1-x}\text{In}_x\text{As}$, the virtual-crystal approximation does not hold on an atomic scale, and that the Ga-As and In-As nearest-neighbor distances do not vary appreciably with the concentration. The next-nearest-neighbor distance shows a broadened single distribution for the cation sublattice, peaked at the averaged lattice distance, and a bimodal distribution for the anions.¹¹

Mixed $\text{GaP}_{1-x}\text{As}_x$ was one of the first mixed-crystal systems in which the ZCP and ZEP vibrational properties have been studied.¹²⁻¹⁷ It has been shown to exhibit a two-mode behavior both for the ZCP's and ZEP's and a model for this, based on the randomness of the P(As) location has been proposed,¹⁰ and a model based on the existence of P(As) clusters was worked out to take into account the observed weak extra structure in the reflectivity spectrum.⁴ The ZCP vibrational properties of $\text{Ga}_{1-x}\text{Al}_x\text{As}$ have been studied;^{10,18} this system shows a two-mode behavior at $\vec{q} \simeq 0$. No weak extra structure has been observed in the restrahlen bands of $\text{Ga}_{1-x}\text{Al}_x\text{As}$.

In this paper we use RS by two-phonon processes to study the crystalline structure of mixed crystals. The phonon density of states is high close to the edge of the zone, and usually the two-phonon Raman spectrum consists of contributions from several zone-edge regions. Since the phase of each ZEP wave changes rapidly from unit cell to unit cell, such phonons should be sensitive both to disorder and to correlation on the scale of a lattice constant. Two sets of mixed crystals will be studied: $\text{GaP}_{1-x}\text{As}_x$ and $\text{Ga}_{1-x}\text{Al}_x\text{As}$, which have different ZEP properties. These different ZEP properties we attribute to structural differences.

II. EXPERIMENTAL RESULTS

RS from mixed $\text{GaP}_{1-x}\text{As}_x$ was performed at room temperature on layers grown by liquid-phase epitaxy on a substrate, which was either GaP for GaP-rich mixed crystals or GaAs for the GaAs-rich ones. The 4880-Å laser wavelength was usually chosen because it is completely absorbed in the (1–3)- μm -thick epitaxial layer. For $x < 0.46$ the crystals have indirect band gaps.¹⁹ In the indirect-gap range phonon replicas were observed for $x \approx 0.2$ and $\lambda = 4880 \text{ \AA}$.²⁰ These (see discussion of Fig. 2) can be avoided by using bulk samples and the 6471-Å krypton-laser line. GaP and GaAs were rendered amorphous by a high implantation dose (10^{15} Sb ions/cm² at room temperature) and then studied using the 4880-Å laser line.

The $\text{Al}_x\text{Ga}_{1-x}\text{As}$ samples were grown by molecular beam epitaxy on a GaAs substrate. For AlAs-rich material the epitaxial layer was covered with a very thin film of GaAs to prevent the deterioration of the mixed crystals. Different laser wavelengths were used in order to avoid resonances. Studies on GaAs (Ref. 21) and $\text{Ga}_{1-x}\text{Al}_x\text{As}$ (Ref. 22) have lead to a model that has the conduction bands at Γ and X crossing for $x \approx 0.4$. For larger concentration x , the conduction-band minima are at X , whereas the valence-band maximum remains at the Γ point.

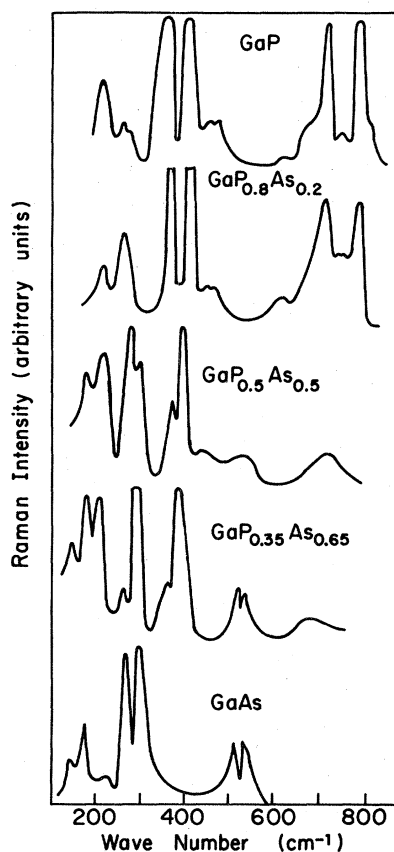


FIG. 1. Room-temperature backscattering Raman spectrum of $\text{GaP}_{1-x}\text{As}_x$ mixed crystals. The laser wavelength is 4880 Å. The scattered light is not analyzed. The crystal plane is perpendicular to the [100] axis.

A. $\text{GaP}_{1-x}\text{As}_x$

Figure 1 shows the Raman spectra of mixed $\text{GaP}_{1-x}\text{As}_x$ crystals excited by the 4880-Å laser line. For all concentrations a two-mode behavior of the ZCP's is observed with two sets of oscillators, one corresponding to GaP and one to GaAs. Combinations of optical ZEP's give Raman peaks in the high-frequency range of the spectrum that can be seen in the frequency range $650 \leq \omega \leq 850 \text{ cm}^{-1}$. These are GaP-like and GaAs-like in the frequency ranges $600 \leq \omega \leq 800 \text{ cm}^{-1}$ and $500 \leq \omega \leq 600 \text{ cm}^{-1}$, respectively. In the concentration range $0 < 1-x \leq 0.65$ the intensity and the width of the GaP-like two-phonon peaks can be conveniently measured without too much error.

In order to compare both the intensity and the line shape of different samples, a backscattering technique has been used: The impinging laser light arrives perpendicular to the crystal and is reflected from a small mirror at the center of the collecting Raman system. For unanalyzed collected light, the Raman efficiency in this case is not dependent on the polarization of the laser with respect to the crystal, and scattering intensities from different samples can be compared.²³ The two-phonon intensity was normalized to the zone center GaP LO intensity multiplied by $1-x$ to take into account the expected dependence of the intensity on the GaP concentration. If the GaP two-phonon intensity were proportional to $(1-x)^2$, this normalized spectrum would be independent of x . Figure 2 shows this normalized GaP two-phonon Raman spectra of $\text{GaP}_{1-x}\text{As}_x$ for different As concentrations, in

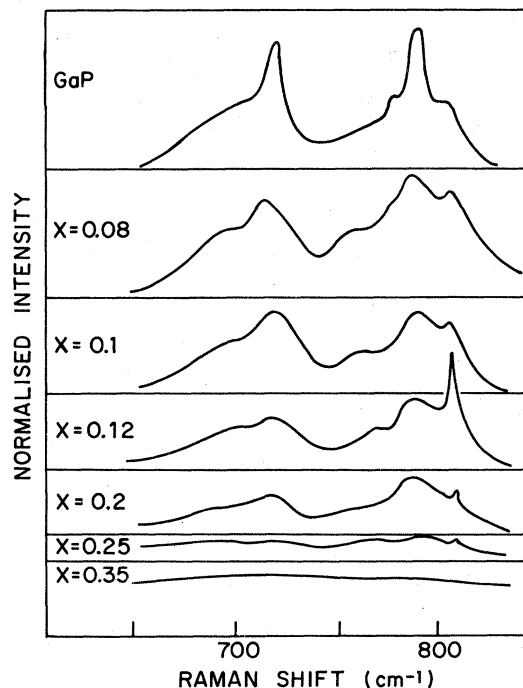


FIG. 2. Room-temperature Raman spectra of $\text{GaP}_{1-x}\text{As}_x$, for different As concentrations. The intensity is normalized to the intensity of the GaP LO $_{\Gamma}$ mode multiplied by $1-x$. The laser wavelength is 4880 Å; the collected light is not analyzed. The crystal plane is perpendicular to the [100] axis.

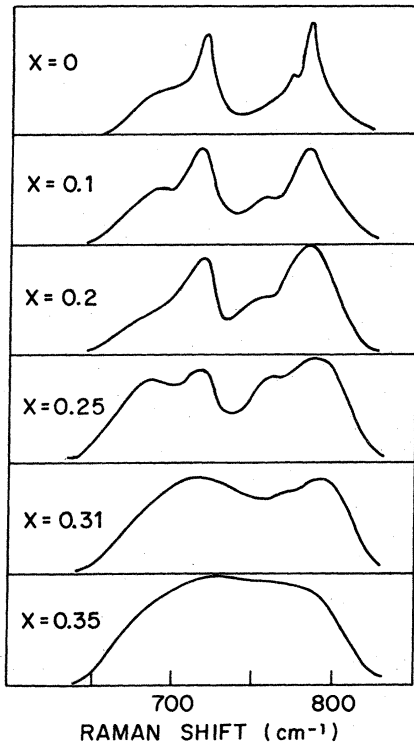


FIG. 3. Line shapes of $\text{GaP}_{1-x}\text{As}_x$ spectra for different As concentrations. The spectra are normalized to the same maximum intensity. The zone-center replicas have been subtracted.

the frequency range $650\text{--}800\text{ cm}^{-1}$. In pure GaP the peaks at 720 and 783 cm^{-1} have $\Gamma_1 + \Gamma_{12}$ symmetry, the structure between these two main peaks has Γ_{15} symmetry and is thus also infrared active.²⁴ In addition to the standard two-phonon Raman spectra, the 2LO_Γ peak is clearly seen for $x \approx 0.2$. This peak has not been used in the comparison of intensities that follows. When the phosphorus concentration decreases in the crystal, the intensity of the GaP ZEP drops very rapidly and the peaks broaden. For concentrations higher than $\approx 25\%$ the peak structure can no longer be singled out and the GaP two-phonon RS spectrum is reduced to a broad and weak band in the frequency range $650 \leq \omega \leq 800\text{ cm}^{-1}$. There was no peak observed in the $(630\text{--}670)\text{-cm}^{-1}$ range that would be the analog of peak C from $\text{Ga}_{1-x}\text{Al}_x\text{As}$ (see below).

Together with the decreases of the Raman intensity, a broadening of the Raman peaks takes place. In Fig. 3, the line shape of the GaP second-order line is shown as a function of As concentration. All of the graphs are normalized to the same maximum intensity. The LO_Γ overtone has been subtracted. When the As impurity concentration is as small as 8%, the spectrum is already appreciably broadened, and when the As concentration reaches $\approx 30\%$ only a single broad two-phonon band remains.

The intensities of the Γ_1 peaks at 720 and 783 cm^{-1} are plotted in Fig. 4; they are normalized to the intensity for $x = 0$. The intensity of these peaks decreases about 2 orders of magnitude when the phosphorus content decreases from 100% to 65%.

These results suggest that even at low concentrations, the As atoms prevent the propagation of GaP vibrations; or, in other words, the GaP two-phonon correlation length

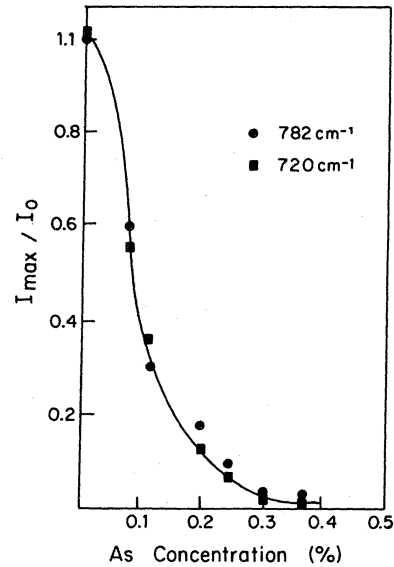


FIG. 4. Concentration dependence of the normalized second-order Raman intensity of the peaks at 718 and 783 cm^{-1} ($\Gamma_1 + \Gamma_{12}$ representation).

is strongly reduced by the presence of As impurities. The nonpolarized two-phonon spectrum is a good picture of the phonon density of states at half the Raman frequency. Our experimental results suggest that when the correlation length is reduced by the disorder, the GaP density of states is broadened by the introduction of As impurities in a way similar to that of amorphous GaP.

If one assumes that in an amorphous solid the vibrational modes can be pictured as nearly localized²⁵ and that the eigenvector envelope may be represented by a plane-wave factor times a spatial damping factor²⁶ $\exp(-r/\Lambda)$, where Λ is the correlation length for phonons, then the Raman intensity is

$$I(\omega) = \sum_b C_b (1/\omega) [n(\omega + 1)] g_b(\omega), \quad (1)$$

where $g_b(\omega)$ is the phonon density of states, $n(\omega)$ is the Bose-Einstein distribution function, and C_b is the coupling constant of the b band. The reduced Raman intensity which can be compared to the phonon density of states is

$$I_R(\omega) = \omega(\omega_L - \omega)^{-4} [n(\omega) + 1]^{-1} I(\omega), \quad (2)$$

where ω_L is the laser frequency. The GaP phonon density of states has been calculated using various models,²⁷ and its agreement with the Raman overtone spectrum^{28,29} is very good. An empirical broadening factor can be extracted from the comparison between the experimental amorphous spectrum and the broadened crystalline density of states.

Figure 5 shows the reduced Raman spectrum of GaP rendered amorphous by heavy ion implantation (dotted-dashed line), together with the two-phonon spectrum at frequency $\omega/2$ (dashed line) and a calculated spectrum (solid line). The calculated spectrum was obtained from the two-phonon spectrum by widening each of the

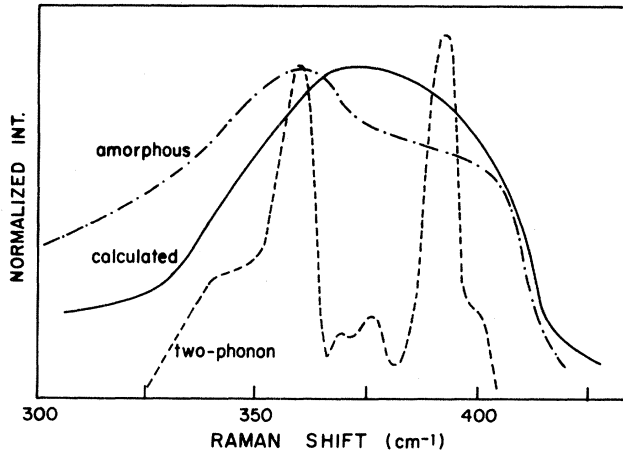


FIG. 5. Reduced Raman spectrum of GaP rendered amorphous by Sb ion implantation as a function of ω , together with the measured two-phonon spectrum at 2ω , along with fit obtained from the two-phonon spectrum broadened by a frequency-independent factor.

density-of-states peaks by a constant factor of 3.8 and plotting the resultant spectrum. The fit has been chosen to be the best on the high-frequency side of the spectrum, because on the low-frequency side acoustical phonons should contribute to the amorphous band. Our experimental data agree with previously published ones.³⁰

As seen in Fig. 6 the width [full width at half maximum (FWHM)] of the phonon density of states, obtained from the Raman two-phonon spectrum, increases roughly linearly with increasing arsenic content. For As concentrations higher than about 30%, the GaP density of states is so broadened and structureless that it compares with the Raman spectrum of amorphous GaP.

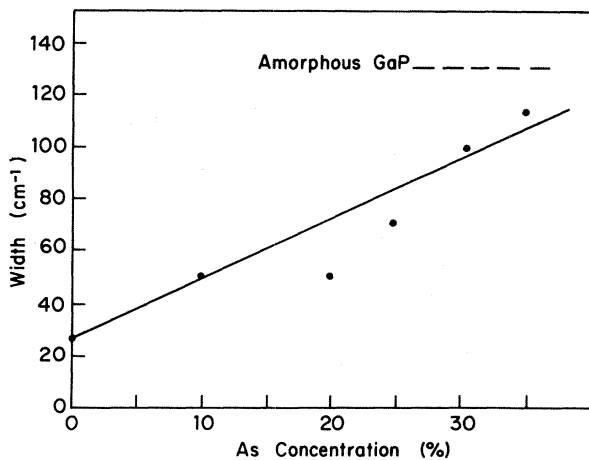


FIG. 6. Width of the density-of-states peak obtained from GaP-like second-order Raman spectra of $\text{GaP}_{1-x}\text{As}_x$, as a function of the As content. The width of the peak from a sample of GaP rendered amorphous by ion implantation is 65 cm^{-1} .

B. $\text{Ga}_{1-x}\text{Al}_x\text{As}$

Figure 7 shows the room-temperature RS of GaAs, AlAs, and some $\text{Al}_x\text{Ga}_{1-x}\text{As}$ crystals. The mixed crystals have a two-mode behavior for the ZCP's. For every concentration we have two sets of normal modes of vibration: TO_1 and LO_1 , which are GaAs-like, and TO_2 and LO_2 , which are AlAs-like. In the backscattering geometry LO_1 and LO_2 are allowed when the incident and scattered polarizations are parallel to the $[110]$ axis; the TO modes are always forbidden. The 5154-\AA Laser line has been used.

In order to have a more detailed examination of the vibrational properties of ZEP's, we shall examine a frequency range $400 \leq \omega \leq 800 \text{ cm}^{-1}$ for different samples. Figure 8 shows the two-phonon RS of different mixed crystals together with the spectra of GaAs and AlAs. The two-phonon spectra of GaAs and AlAs materials are in accordance with the published results. GaAs exhibits two

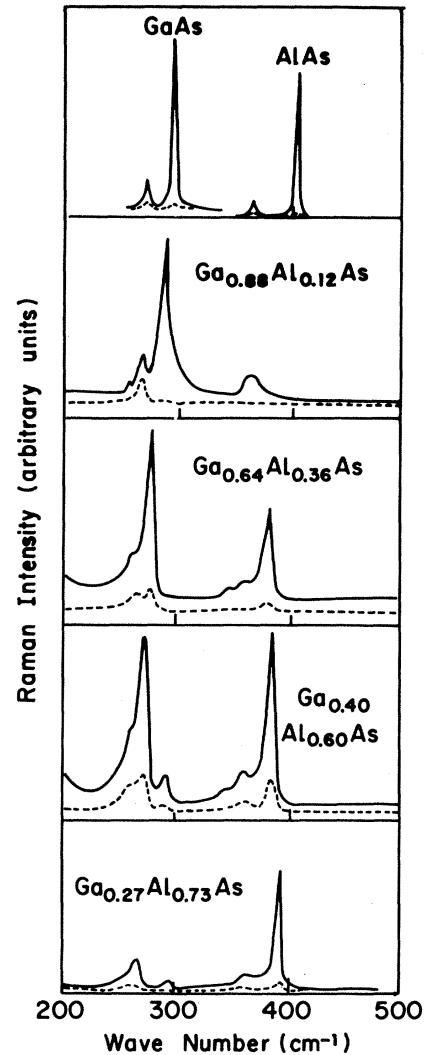


FIG. 7. Raman spectra of GaAs, AlAs, and mixed $\text{Ga}_{1-x}\text{Al}_x\text{As}$. The laser excitation wavelength is 5154 \AA . The crystal plane is perpendicular to the $[100]$ axis. The incoming light polarization vector is parallel to the $[110]$ axis and the outgoing polarization is either parallel (solid line) or perpendicular ($[1\bar{1}0]$ to this axis (dashed line)).

main peaks: $2TO(X,K)$ at 503 cm^{-1} and $2TO(L)$ at 532 cm^{-1} .³¹ The AlAs two-phonon band extends from 670 to 800 cm^{-1} with a well-defined $2TO_X$ peak at 691 cm^{-1} .³²

As long as the aluminum content is small ($x \leq 30\%$) the two-phonon spectrum is very much like that of GaAs, the peaks tending to blur with increasing x . The intensity of the two-phonon spectrum normalized to that of LO_1 , remains roughly constant. When $x = 36.5\%$ the two-phonon RS is composed of four bands: the *A* band, $420 \leq \omega \leq 480\text{ cm}^{-1}$; the *B* band, $480 \leq \omega \leq 560\text{ cm}^{-1}$; the *C* band, $560 \leq \omega \leq 670\text{ cm}^{-1}$; and the *D* band, $670 \leq \omega \leq 800\text{ cm}^{-1}$. The *B* band is GaAs-like but without the structure seen in the pure material. The *D* band is AlAs-like, but the sharp $2TO(X,K)$ peak has disappeared. In addition to these two bands, which are found in any two-mode behavior mixed crystals, two additional bands are seen. The one labeled as *C* between the GaAs-like and the AlAs-like two-phonon bands is clearly due to combinations of GaAs plus AlAs optical ZEP's. Prior to publication of this paper such a combination

band had not been seen in any nonresonant two-mode behavior mixed crystal. The *A* band, which does not appear in GaAs, is due to combinations of acoustical and optical phonons of GaAs and AlAs. The intensity of the *B* band, normalized to the LO_1 one, does not vary with x , contrary to what has been observed for $GaP_{1-x}As_x$.

For $x = 60\%$ the spectrum is similar to that of $Ga_{0.73}Al_{0.27}As$, with the four bands clearly defined. In order to make sure that we were not under resonant conditions, we used other laser wavelengths and we obtained the same results.

III. DISCUSSION

Because the wave vector of the light \vec{k}_0 is very small on the scale of a reciprocal-lattice vector the phonon wave vectors \vec{q}, \vec{q}' obey either $\vec{q} = -\vec{q}' \approx \vec{0}$ or $\vec{q} - \vec{q}' = \vec{0}$. The first process is usually weak, because the phonon density of states is small at the center of the Brillouin zone. Two ZEP's of a well-defined wave vector can combine only if the condition $\vec{q} = -\vec{q}'$ is fulfilled. How stringent this condition is remains to be understood.

GaP, GaAs, and AlAs have the zinc-blende structure. As seen in Table I the lattice constants and the force constants of GaAs and AlAs are very similar, but they are quite different for GaP and GaAs.

Discussions of all the previous published data have been made by assuming that the atoms are randomly distributed on the Ga-Al sublattice. Evidence for this includes the absence of structure in the infrared reflectivity spectra¹⁰ and absence of excitons bound to fluctuations of the periodic potential.⁹ On the other hand, such features are present in the infrared and the photoluminescence spectra of $GaP_{1-x}As_x$ and have been explained by assuming deviations from a randomly distributed material.^{4,8}

If we assume that the Ga-Al disorder in $Ga_{1-x}Al_xAs$ is completely random, the correlation range for the disorder is only a nearest-neighbor distance. The mechanical effect of the disorder is due primarily to the Ga-Al atom mass difference, since the force-constant change and bond-angle variations are small. Now consider the driven response of the lattice to a ZEP, for example, $LO(X)$. Alternate Ga-Al planes normal to $[100]$ will be driven with a π phase shift, but the fluctuations in the masses on those planes will make it impossible for the As atoms on adjacent planes to remain at rest as they would for an $LO(X)$ mode in GaAs or AlAs. Because of this, because of the essentially zero correlation length for disorder, and because of the staggering of the tetrahedral bonds, we expect that this mode will have a doubly peaked spectral density and that a given GaAs bond (or an AlAs bond) will participate in vibrations at both the GaAs-like and the AlAs-like ZEP frequency. The two-phonon spectrum induced by a second-order polarizability derivative on bonds that link Ga-Al planes with As planes will then have three peaks corresponding to the two overtones and the one combination.

The nonfulfillment of the momentum conservation in mixed $GaP_{1-x}As_x$ should account for the nonappearance of cross coupled GaP-like and GaAs-like ZEP. The broadening and the decrease in the GaP two-phonon in-

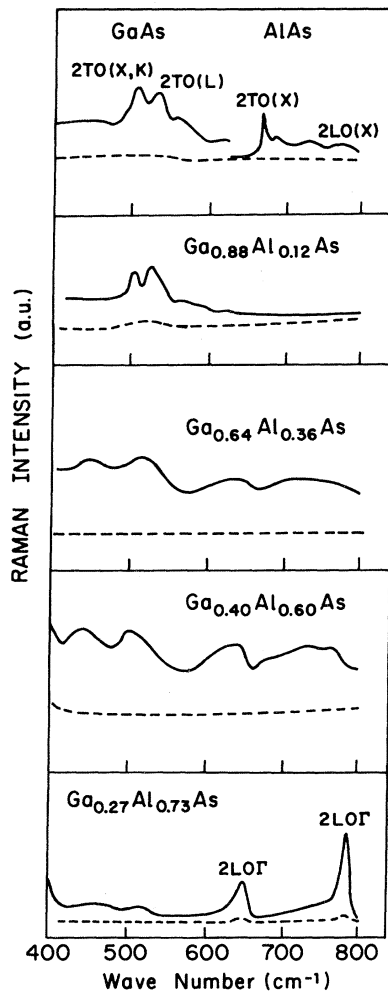


FIG. 8. Two-phonon Raman spectra of GaAs, AlAs, and mixed $Ga_{1-x}Al_xAs$. Laser wavelength is 5154 \AA . The polarization vector of the incident light is parallel to the $[100]$ axis and the scattered light is either parallel (solid line) or perpendicular ($[010]$) to this axis (dashed line).

TABLE I. Material parameters (these values are taken from Refs. 10 and 4).

	GaP	GaAs	AlAs
Lattice constant (Å)	5.4495	5.6419	5.6611
Nearest-neighbor central-force constant (dyn/cm)	19.62×10^9	17.81×10^9	18.11×10^9

tensity with increasing As concentration can be accounted for by at least two assumptions which do not exclude each other. We could have local clustering of P or As atoms around Ga atoms and/or we could have a local distortion of the lattice due to tetrahedral bond-angle variations that necessarily follow from lattice mismatch. The second assumption is in accordance with the recent EXAFS experiments.¹¹ These two assumptions are not contradictory, and it seems likely that some departure from a purely random system, as well as distortions of the lattice occur in crystals such as $\text{GaP}_{1-x}\text{As}_x$. As pointed out earlier, the appearance of cross coupled two-phonon peaks in $\text{Ga}_{1-x}\text{Al}_x\text{As}$ mixed crystals, and the constant two-phonon intensity with increasing x , are typical features of these mixed crystals where good lattice matching exists. It should be noted using thermodynamic arguments that $\text{Ga}_{1-x}\text{Al}_x\text{As}$ is less likely to have excess free energy than $\text{GaP}_{1-x}\text{As}_x$,³⁴ and therefore less likely to form clusters.

In order to understand the broadening and the decrease of the two-phonon peak intensities of $\text{GaP}_{1-x}\text{As}_x$, we assume that phosphorus and arsenic atoms are not completely randomly distributed. Some areas in the crystal are more GaP or GaAs rich than the average crystal. In each GaP-rich area, GaP-like phonons are generated which decay exponentially in the GaAs-rich area.

The intensity I of the two-phonon RS at frequency shift ω is proportional to the \vec{q} th spatial Fourier transform of the correlation function of the second-order fluctuation in the dielectric constant $\delta^{(2)}\epsilon(\vec{r}, t)$:

$$I \propto \int \langle \delta\epsilon^{(2)}(\vec{r}', t') \delta\epsilon^{(2)}(\vec{r} + \vec{r}', t + t') \rangle_{r', t'} \times e^{i(\vec{q} \cdot \vec{r} - \omega t)} d^3r dt.$$

Here \vec{q} is the wave-vector transfer. In random media one often assumes that the spatial part of the correlation function takes the form

$$\langle \delta\epsilon^{(2)}(\vec{r}', t') \delta\epsilon^{(2)}(\vec{r} + \vec{r}', t + t') \rangle_{r', t'} \propto e^{-r/\Lambda}.$$

For a correlation length Λ short compared with $2\pi/q$, we

then obtain

$$I \propto \Lambda^3.$$

Thus the intensity should be proportional to the correlation volume for second-order fluctuations.

When the arsenic concentration in $\text{GaP}_{1-x}\text{As}_x$ reaches $x \approx 0.30$, the two-phonon linewidth is that of amorphous GaP at twice the Raman frequency. The correlation length for amorphous GaP is about 20 Å, which is the extent of Λ for a two-phonon mode with $x \approx 0.30$. The Raman intensity of crystalline GaP is about 2 orders of magnitude higher than in $\text{GaP}_{0.7}\text{As}_{0.3}$; an order-of-magnitude estimate for the correlation length of GaP ZEP's should then extend to ≈ 90 Å.

The perturbations in the random distribution of atoms are small in size, and the crystal remains roughly periodic. The correlation length of the zone-center normal mode of vibrations TO_{Γ} and LO_{Γ} extends above 1000 Å. This explains why ZCP are less sensitive to fluctuations in the random distribution of atoms, although these phonons can be used to monitor damage on the scale of 1000 Å such as produced by poor polishing³⁵ or poor crystalline quality.³⁶

IV. CONCLUSIONS

Two types of behavior have been observed for the ZEP's of $\text{Ga}_{1-x}\text{Al}_x\text{As}$ and $\text{GaP}_{1-x}\text{As}_x$ mixed crystals. $\text{Ga}_{1-x}\text{Al}_x\text{As}$ ZEP's show combinations between the GaAs and the AlAs branches which is not the case for $\text{GaP}_{1-x}\text{As}_x$. In the latter case, the width of the overtone peaks increases rapidly with x , and the intensity decreases rapidly. These results have been interpreted by assuming that in $\text{Ga}_{1-x}\text{Al}_x\text{As}$ the atoms are randomly distributed, which is not the case for mixed $\text{GaP}_{1-x}\text{As}_x$ materials.

ACKNOWLEDGMENTS

The work at the University of Illinois was supported by the U.S. Joint Services Electronics Program under Contract No. N00014-79-C-0424 and the National Science Foundation under the Materials Research Laboratories Program DMR-80-20250.

¹R. J. Elliott, J. A. Krumhansl, and P. L. Leath, Rev. Mod. Phys. **46**, 465 (1974).

²I. F. Chang and S. S. Mitra, Adv. Phys. **20**, 353 (1971).

³R. Beserman and M. Balkanski, Phys. Rev. B **1**, 608 (1970).

⁴H. W. Verleur and A. S. Barker, Phys. Rev. **149**, 715 (1966).

⁵H. Kawamura, R. Tsu, and L. Esaki, Phys. Rev. Lett. **29**, 1397 (1972).

⁶Z. Vardeny and O. Brafman, Phys. Rev. B **12**, 3290 (1979).

⁷D. N. Talwar, M. Vandevyer, and M. Zigone, J. Phys. C **13**, 3775 (1980).

⁸Shui Lai and M. V. Klein, Phys. Rev. Lett. **44**, 1087 (1980).

⁹Shui Tong Lai, Ph.D. thesis, University of Illinois at Urbana-Champaign, 1980.

¹⁰O. K. Kim and W. G. Spitzer, J. Appl. Phys. **50**, 4362 (1979).

¹¹J. C. Mikkelsen, Jr. and J. B. Boyce, Phys. Rev. Lett. **49**, 1912 (1982).

¹²Y. S. Chen, W. Shockley, and G. L. Pearson, Phys. Rev. **151**, 648 (1966).

¹³R. Beserman and D. Schmeltzer, Solid State Commun. **24**, 793 (1977).

- ¹⁴R. Beserman, *Solid State Commun.* **23**, 323 (1977).
- ¹⁵D. Schmeltzer, R. Beserman, and D. Slamovits, *Phys. Rev. B* **22**, 4038 (1980).
- ¹⁶N. D. Strahm and A. L. McWhorter, in *International Conference on Light Scattering*, edited by G. B. Wright (Springer, New York, 1968), p. 455.
- ¹⁷D. Schmeltzer and R. Beserman, *Phys. Rev. B* **22**, 6330 (1980).
- ¹⁸M. Illegems and G. L. Pearson, *Phys. Rev. B* **1**, 1576 (1970).
- ¹⁹A. Onton and L. M. Foster, *J. Appl. Phys.* **43**, 5084 (1972).
- ²⁰D. Schmeltzer and R. Beserman, *J. Phys. C* **14**, 273 (1981).
- ²¹D. E. Aspnes, C. G. Olson, and D. W. Lynch, *Phys. Rev. Lett.* **37**, 766 (1976).
- ²²R. Dingle, R. A. Logan, and J. R. Arthur, Jr., *Proceedings of the 6th International Symposium on Gallium Arsenide and Related Compounds* (IOP, London, 1977), p. 210.
- ²³P. A. Temple and C. E. Hathaway, *Phys. Rev. B* **7**, 3685 (1973).
- ²⁴B. A. Weinstein and M. Cardona, *Solid State Commun.* **10**, 361 (1972).
- ²⁵R. J. Bell, *Rep. Progr. Phys.* **35**, 1315 (1972).
- ²⁶R. Shuker and R. Gammon, *Phys. Rev. Lett.* **25**, 222 (1970); in *Proceedings of the 2nd International Conference on Light Scattering in Solids, Paris 1971*, edited by M. Balkanski (Flammarion, Paris, 1971), p. 334.
- ²⁷K. Kunc, M. Balkanski, and M. A. Nusimovici, *Phys. Status Solidi* **72**, 223 (1975).
- ²⁸E. S. Koteles and W. R. Datars, *Solid State Commun.* **19**, 221 (1976).
- ²⁹R. L. Schmidt, K. Kunc, M. Cardona, and H. Bilz, *Phys. Rev. B* **20**, 3345 (1979).
- ³⁰M. Wihl, M. Cardona, and J. Tauc, *J. Non-Cryst. Solids* **8-10**, 172 (1972).
- ³¹R. Trommer, E. Anastassakis, and M. Cardona, in *International Conference on Light Scattering in Solids*, edited by M. Balkanski, R. C. C. Leite, and S. P. S. Porto (Flammarion, Paris, 1975), p. 396.
- ³²P. B. Klein, Jin-Joo Song, and R. K. Chang, in *International Conference on Light Scattering Solids*, Ref. 31, p. 93.
- ³³D. E. Aspnes, S. M. Kelso, C. G. Olsen, and D. W. Lynch, *Phys. Rev. Lett.* **48**, 1862 (1982).
- ³⁴B. de Cremoux, *J. Phys. (Paris) Colloq.* **43**, C5-19 (1982).
- ³⁵D. J. Evans and S. Ushioda, *Phys. Rev. B* **9**, 1638 (1974).
- ³⁶P. Parayanthal, F. H. Pollak, and J. M. Woodall, *Appl. Phys. Lett.* **41**, 361 (1982).